Published online August 9, 2007

Magnetic Enhancement and Iron Oxides in the Upper Luochuan Loess–Paleosol Sequence, Chinese Loess Plateau

José Torrent*
Departamento de Ciencias y Recursos Agrícolas y Forestales
Universidad de Córdoba
Edificio C4, Campus de Rabanales
14071 Córdoba
Spain

Qingsong Liu
School of Ocean and Earth Science
National Oceanography Centre
Univ. of Southampton
European Way
Southampton SO14 3ZH
UK

Jan Bloemendal
Dep. of Geography
Roxby Building
Univ. of Liverpool
Liverpool L69 7ZT
UK

Vidal Barrón
Departamento de Ciencias y Recursos Agrícolas y Forestales
Universidad de Córdoba
Edificio C4, Campus de Rabanales
14071 Córdoba
Spain

Variations in the low-field magnetic susceptibility of the wind-blown Chinese Loess Plateau (CLP) loess–paleosol sequences reflect changes in the global paleoclimate on different time scales. Magnetic enhancement in paleosols has been ascribed to the neoformation of fine-grained maghemite; however, little is known about the pathway through which this mineral was formed in the CLP paleosols, its relationships with the other pedogenic Fe oxides (viz. hematite and goethite), and the pedoclimatic significance of such relationships. In this work, we characterized various magnetic, chemical, and mineralogical properties of the loess–paleosol units at depths from about 23 to 55 m in the Upper Luochuan section, central CLP. The concentration of pedogenic hematite (ΔHm) and the frequency-dependent magnetic susceptibility (χ_{FD}), which is used as a proxy for the concentration of fine-grained pedogenic maghemite, were found to be linearly correlated (R^2 = 0.825, P < 0.001). This supports the idea that these two minerals were formed concomitantly during pedogenesis, which is consistent with the results of previous in vitro experiments showing that the ferrihydrite → maghemite → hematite transformation takes place under aerobic conditions. By contrast, the concentration of pedogenic goethite (ΔGt) was only weakly correlated with either χ_{FD} or ΔHm, which suggests that goethite formed through an alternative pathway. The paleosols above 40 m (S4, S5, corresponding to marine isotope stages 9 and 11, respectively) exhibit a higher degree of weathering and higher ΔHm/(ΔHm + ΔGt) ratio than those below such a depth (S6–S8). This was ascribed to differences in paleoclimatic conditions, which are moister and warmer in the former paleosols than in the latter, rather than to differences in pedogenesis duration.

Abbreviations: CLP, Chinese Loess Plateau; Fe_d, citrate–bicarbonate–dithionite-extractable iron; Fe_t, total iron; GSD, grain size distribution; Gt and Hm, goethite and hematite concentrations, respectively; PSD, pseudo-single domain; SD, single domain; SP, superparamagnetic; ΔGt and ΔHm, pedogenic goethite and hematite concentration, respectively; χ_{ARM}, anhysteretic remanent magnetization susceptibility; χ_{FD}, frequency-dependent mass magnetic susceptibility; χ_{HF}, high-frequency magnetic susceptibility; χ_{LF}, low-frequency magnetic susceptibility.

SOIL MINERALOGY

Global glacial–interglacial paleoclimate cycles are unambiguously substantiated by the interbedded wind-blown loess–paleosol sequences in the CLP (Heller and Liu, 1984, 1986; Kukla et al., 1988; Deng et al., 2006). The loess units were deposited during cold and dry glacial periods and the paleosols were formed by the in situ alteration of the parent loess (i.e., the "aeolian input" with a reduced sedimentation rate) during warm and humid interglacial periods. These paleosols are magnetically enhanced as the result of the neoformation of ferrimagnetic minerals (Zhou et al., 1990; Maher and Thompson, 1992; Liu et al., 2005). Some weathering of the aeolian inputs occurred during transportation, as suggested by the presence of significant amounts of goethite and hematite in the parent loess (Balsam et al., 2004). The effects, however, are slight, especially if one considers the magnetic contrasts between loess and paleosol units (a strong connection exists between magnetic susceptibility per unit mass, χ, and the degree of pedogenesis; see Maher et al., 1994; Vidic et al., 2004; and references therein).

The main phase accounting for magnetic enhancement is maghemite in the superparamagnetic (SP, <20–25 nm) and single-domain (SD, between 20–25 and ~100 nm) grain size regions (Fine et al., 1993; Verosub et al., 1993; Heller and Evans, 1995; Liu et al., 2005). The role of both SP and SD particles has been discussed in a number of studies (e.g., Geiss and Zanner, 2006, and references therein). Although SP maghemite exhibits inherently higher magnetic susceptibility values than does SD maghemite, the latter seems to contribute substantially to the

Soil Sci. Soc. Am. J. 71:1570–1578
doi:10.2136/sssaj2006.0328
Received 15 Sept. 2006.
*Corresponding author (torrent@uco.es).

total bulk magnetic susceptibility by virtue of its increased volume percentage (Liu et al., 2004b). It can therefore be concluded that the magnetic enhancement of paleosols is caused by the neoformation of pedogenic, fine-grained (SP + SD) maghemite, which, in contrast to the coarse ferrimagnetic particles present in the parent loess, is soluble in a citrate–bicarbonate–dithionite mixture (Verosub et al., 1993).

Because the CLP local climate (which is reflected, for example, in χ) and the global climate (as represented, for example, by the marine O-isotope records) are related, the corresponding proxies have been extensively correlated (Heller and Liu, 1984, 1986; Balsam et al., 2005; and references therein). Moreover, χ has been further used to quantify variations in the amount of paleorainfall (Maher et al., 2003, and references therein). The contention that paleorainfall is the main factor affecting χ has been qualified, however, by studies that suggest the influence of soil temperature and the duration of pedogenesis (Maher, 1998; Fine et al., 1989; Vidic and Verosub, 1999; Vidic et al., 2004). Because the latter factors obviously affect other soil properties (e.g., clay, carbonate, and Fe oxide contents and color), a multiproxy approach is preferable with a view to reconstructing the nature of paleoclimates (Balsam et al., 2004; Vidic et al., 2004).

Interpreting the magnetic enhancement data for paleosols is complicated by the uncertainty in the relative significance of the different pathways from Fe-bearing minerals to maghemite in soils. As discussed by Cornell and Schwertmann (2003), maghemite can be formed by oxidation of detrital magnetite and or by thermal (fire) transformation of other Fe oxides [a term that is used here to designate all Fe(III) oxides, oxyhydroxides, and hydroxides]. It has also been hypothesized that, under reducing conditions—which determine the presence of Fe^{2+} in solution—magnetite is formed abiotically (Maher and Taylor, 1988) or by bacterial mediation (Fassbinder et al., 1993; Lovley et al., 1987; Chen et al., 2005), and later oxidized to maghemite with the onset of oxidizing conditions (van Velzen and Dekkers, 1999; Liu et al., 2003, 2004a). Recently, the hypothesis has been put forward that maghemite is an intermediate in the transformation of ferrihydrite—which is considered to be the first product of the weathering of Fe-bearing minerals—to hematite in aerobic soils (Barrón and Torrent, 2002; Barrón et al., 2003; Torrent et al., 2006). This is supported by the covariance of χ and hematite concentration in several CLP sections and in soil profiles on loess and other parent materials in various world regions (Torrent et al., 2006).

One other problem is the relationship between the concentration of maghemite and those of hematite (Hm) and goethite (Gt), which are the main Fe oxides produced in the course of pedogenesis. It is well established that the Hm/(Hm + Gt) ratio is highly dependent on the particular pedoenvironment, with colder, moister, more acidic, organic-matter-rich environments favoring goethite over hematite (Schwertmann, 1985). Balsam et al. (2004) related this ratio to χ and other paleoclimatic indicators in the Luochuan and Lingtai sections of the CLP. These researchers hypothesized that, above certain rainfall and temperature thresholds, hematite, goethite, and magnetite (which is subsequently oxidized to maghemite) are formed; with increasing rainfall (and temperature), the ratio of magnetite to hematite increases because the duration of the relatively dry period needed for the dehydration of ferrihydrite to hematite decreases and the duration of the anaerobic period [needed for reduction of Fe(III) to Fe(II) and subsequent formation of magnetite] also increases. With a further increase in rainfall, hematite is no longer produced. Eventually, if the soil is saturated with water (i.e., under anaerobic conditions) for long periods, one can expect Fe oxides to be reductively dissolved and the soil to become depleted in Fe (Bigham et al., 2002). Balsam et al. (2004) also found that the Hm/(Hm + Gt) ratio had steadily decreased in the last 2.5×10^6 yr, which suggests a change in the timing of precipitation, in temperature, or in both.

The first aim of the present work was to characterize in detail the relationships between the concentrations of pedogenic hematite, goethite, and fine-grained maghemite in the upper part of the Luochuan loess–paleosol sequence. For this purpose, pedogenic maghemite was represented by the frequency-dependent susceptibility, χ_{FD}, defined as $\chi_{LF} - \chi_{HF}$, where χ_{LF} and χ_{HF} are the values of χ measured at low and high frequency, respectively. Such relationships were then used (i) to validate the various models proposed to explain the formation of the different Fe oxides, and (ii) to identify the paleoenvironmental differences responsible for the mineralogical differences among paleosols. Finally, several unresolved questions concerning the proposed pedogenic models were addressed.

MATERIALS AND METHODS

Sampling

Samples were collected in the Luochuan section (about 135 m in thickness at 35.8° N, 108.6° E; Bloemendal and Liu, 2005), which is located in the central part of the CLP (Fig. 1) and has a current mean annual precipitation of ~570 mm and mean annual temperature of ~9.8°C. The surface ~50-cm sediments were removed before sampling. The depth interval studied was about 23 to 55 m, which, according to the conventional notation used in the CLP (Bronger, 2003), comprises the following sequence of loess (L) and paleosol (S) units: L4–S4–L5–S5–L6–S6–S7–S8–L9 (Fig. 2). The soil units consist mainly of rubified Bw and Bt horizons underlain by Ck horizons (Bronger, 2003). Samples were collected at 5-cm intervals and stored in polyethylene bags. All were used for magnetic measurements and 53 of them, spaced in accordance with the changes observed in magnetic properties, were used for comprehensive chemical and mineralogical analysis.

Magnetic Measurements

The value of χ, expressed here in 10^{-6} m^3 kg^{-1}, was measured at two frequencies (LF = 0.47 kHz and HF = 4.7 kHz) with a Bartington MS 2B dual-frequency sensor (Bartington Instruments Ltd., Oxford, UK) and the frequency-dependent susceptibility, χ_{FD}, was then calculated as $\chi_{LF} - \chi_{HF}$. This parameter is sensitive only to a very narrow grain size region crossing the SP/SD threshold (~20–25 nm for maghemite) (Worm and Jackson, 1999). For natural samples, however, which generally exhibit a continuous and nearly constant grain size distribution (GSD), χ_{FD} can be used as a proxy for relative changes in concentration in pedogenic fine-grained magnetic particles (Liu et al., 2005; see below). The relative χ_{FD} (χ_{FD}% defined as $100 \times \chi_{FD}/\chi_{LF}$) was then calculated to determine the relative variations in GSD of pedogenic maghemite particles.

Anhysteretic remanent magnetization (ARM) was imparted by using a peak alternating field of 100 mT with a biasing field of 40 μT. The ARM is particularly sensitive to the content of stable single-domain (typically larger than 20–25 nm, but less than ~100 nm for maghemite) ferrimagnets (Dunlop and Özdemir, 1997). In what follows, ARM is expressed as ARM susceptibility (χ_{ARM} = ARM/40 μT).

The combined frequency (1 and 10 Hz in fields of ~240 A m^{-1}, or 0.3 mT) and low-temperature dependence (10–300 K) of suscep-

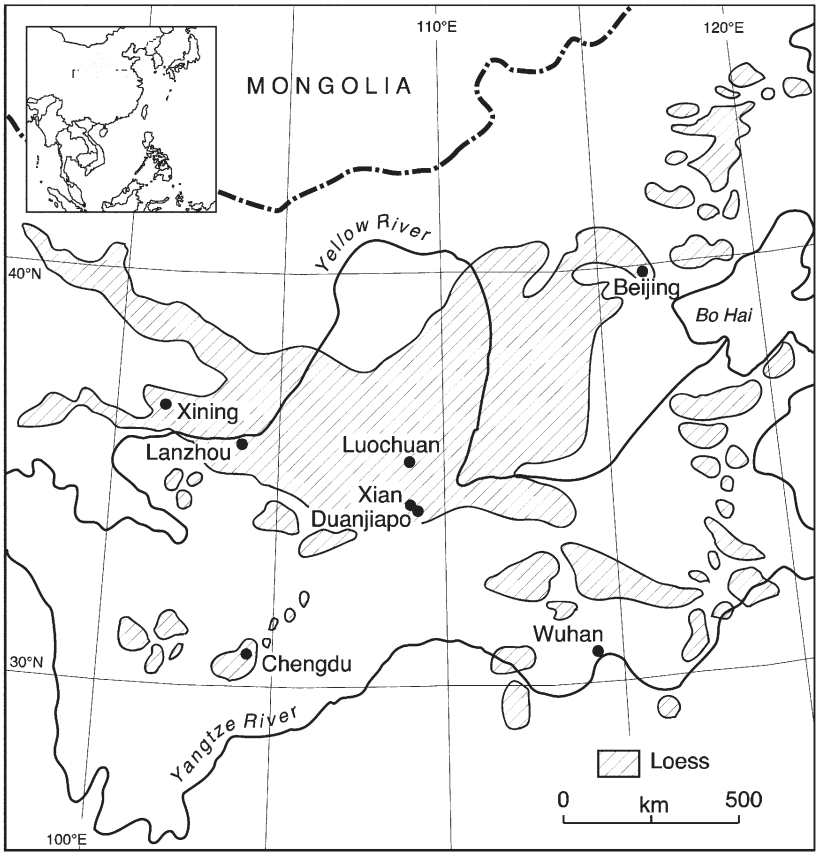

Fig. 1. Distribution of the Chinese Loess Plateau and site location.

tibility curves (hereafter referred to as $\chi_{FD} - T$, where $\chi_{FD} = \chi_{1Hz} - \chi_{10Hz}$ and T represents temperature) for samples at depths of 32.0, 33.5, and 37.2 m were measured using a Quantum Design Magnetic Properties Measurement System (Quantum Design, San Diego, CA). These samples were selected on the basis of their distinct bulk magnetic susceptibility across the S5–L6 boundary.

Diffuse Reflectance Spectroscopy Measurements and Calculations

Diffuse reflectance spectra were recorded from 380 to 900 nm in 0.5-nm steps at a scan rate of 30 nm min^{-1}, using a Varian Cary 1E spectrophotometer equipped with a $BaSO_4$–coated integrating sphere 73 mm in diameter (Varian Inc., Palo Alto, CA). Samples were previously powdered (<10 μm) and pressed by hand into the 8- by 17-mm rectangular holes of white plastic holders (thickness 2.5 mm) at a pressure >500 kPa. The resulting mounts were self supporting, thus allowing the holders to be vertically placed without the powder falling into the sphere. The Kubelka–Munk (K–M) remission function [$F(R_\infty)$] at each wavelength was calculated from

$$F(R_\infty) = \frac{K}{S} = \frac{(1-R_\infty)^2}{2R_\infty} \quad [1]$$

where K and S are the absorption and scattering coefficients, respectively, as defined in the K–M theory, and R_∞ is the reflectance of a thick layer of sample (~1–2 mm for samples containing Fe oxides). The first and second derivatives of the K–M function were calculated by using a cubic spline procedure. This method involves end-to-end joining of a number of cubic polynomial segments based on a certain number of adjacent data points with continuity in the first and second derivative at the joints. Segments with 30 data points were adopted because they provided second-derivative spectra with both well-resolved absorption bands and relatively low background noise.

The difference in ordinate between the minimum and the next maximum at a longer wavelength, which is hereafter referred to as *band intensity*, was used as a proxy for the true band amplitude (Scheinost et al., 1998). The intensities of the bands at ~425 nm (I_{425}) and ~535 nm (I_{535}) are proportional to the concentration of goethite and hematite, respectively (Scheinost et al., 1998), and can thus be used as proxies for relative changes in the mass concentration of goethite and hematite.

The concentrations of goethite and hematite were then quantified with two methods. One was based on the following calibration curve:

$$Y = -0.133 + 2.871X - 1.709X^2 \quad [2]$$

Such a curve, where Y is the Hm/(Hm + Gt) ratio and X is the $I_{535}/(I_{425} + I_{535})$ ratio, was constructed from 22 samples of soils from the Mediterranean region (A and B horizons of Alfisols and Inceptisols of variable age and contents in goethite and hematite). The "true" concentrations of hematite and goethite in the samples were determined by differential x-ray diffraction. Equation [2] accounted for 90% of the variance in Y and held at $0.07 < X < 0.4$, a condition which was fulfilled by the studied loess and paleosol samples. The mass concentrations of hematite and goethite were estimated from Y by assigning all citrate–bicarbonate–dithionite (CBD)-extractable Fe (Fe_d) to these two minerals. The contribution of ferrihydrite to Fe_d was neglected because oxalate-extractable Fe, which provides an estimate of the ferrihydrite concentration, was typically <8% of Fe_d. The mass contribution of maghemite, which is also dissolved by CBD, was also neglected on the basis of the results of Liu et al. (2004b). These

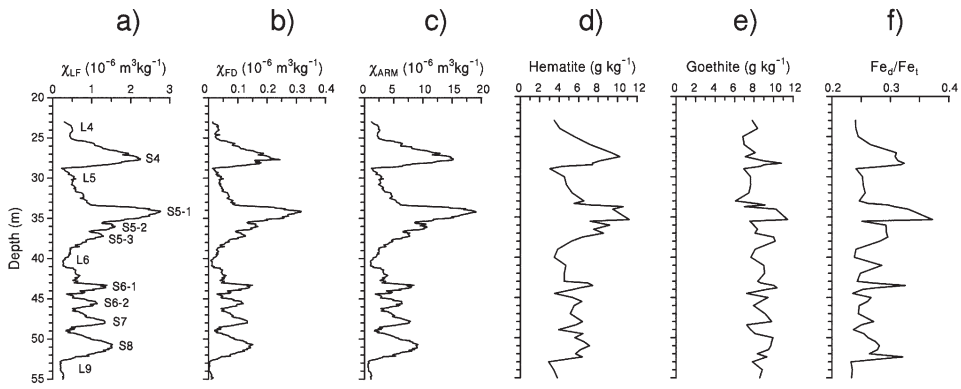

Fig. 2. Depth plots of (a) low-frequency magnetic susceptibility, χ_{LF}; (b) frequency-dependent magnetic susceptibility, χ_{FD}; (c) anhysteretic remanent magnetization susceptibility, χ_{ARM}; (d) hematite concentration; (e) goethite concentration; and (f) dithionite-extractable Fe/total Fe ratio (Fe_d/Fe_t). Gray bars and S notations denote the paleosols and L notations the loess units.

researchers showed the saturation magnetization (M_s) of a Yuanbao paleosol sample with a bulk susceptibility of 1.3×10^{-6} m^3 kg^{-1} to be only 0.05 A m^2 kg^{-1}. After correcting for the contribution from the parent loess (~0.02 A m^2 kg^{-1}), the mass concentration of pedogenic maghemite was ~0.4 g kg^{-1}, which is much smaller than Fe_d in comparable samples in the present study (>10 g kg^{-1}). Therefore, for simplicity, we assigned Fe_d to the combination of Fe in stoichiometric hematite and goethite:

$$Fe_d = Hm/1.43 + Gt/1.59 \quad [3]$$

and calculated the concentrations of hematite and goethite from Eq. [2] and [3].

The second method was based on the following regression equation:

$$Fe_d = GI_{424} + HI_{535} \quad [4]$$

where the regression coefficients G (8.56×10^3) and H (22.2×10^3) represent the factors by which I_{424} and I_{535} must be multiplied to estimate the portion of Fe_d (in mg kg^{-1}) pertaining to goethite and hematite, respectively. This equation was obtained from the value of Fe_d and the spectral data for the 83 CLP loess and paleosol samples studied by Torrent et al. (2006), and was similar to that based on the 53 samples used in the present study. Based on the respective stoichiometric factors, the estimated concentration of goethite was $1.59GI_{424}$ and that of hematite was $1.43HI_{535}$. From these values, we calculated the Hm/(Hm + Gt) ratio and then recalculated the absolute concentrations of hematite and goethite using Eq. [3].

Based on the good correlations between the estimates provided by the two methods [Hm(Method 2) = 0.81 + 0.846Hm(Method 1); R^2 = 0.994; n = 53, P < 0.001; Gt(Method 2) = 1.16 + 0.883Gt(Method 1); R^2 = 0.873; n = 53, P < 0.001], the average value was finally adopted for both hematite and goethite.

Chemical Analyses

Samples (ground to <2 mm) were analyzed for Fe_d by the method of Mehra and Jackson (1960), except that extraction temperature was 25°C and the extraction time 16 h. Oxalate-extractable Fe was determined by using the method of Schwertmann (1964), which involves one 2-h extraction with 0.2 *M* ammonium oxalate at pH 3. The total concentrations of Fe (Fe_t) and other elements were determined by isotope-source x-ray fluorescence, using a Metorex XMET920 system (Metorex International Oy, Espoo, Finland) with a 3 to 20 keV probe (^{109}Cd source). Spectra were deconvoluted using the in-house PASCAL software DECONV (Boyle, 2000) and calibrated using standard samples of known elemental concentration.

Expressing the concentrations of hematite and goethite on a carbonate-free basis required estimating the mass concentration of $CaCO_3$ equivalent in the sample, which was calculated by multiplying by a stoichiometric factor of 2.5 the total concentration of Ca less the mean Ca concentration in carbonate-free samples (~6 g kg^{-1}).

As noted above, we used Fe_d as a measure of Fe present in the Fe oxides, and the Fe_d/Fe_t ratio as an index of the degree of weathering of Fe-bearing minerals in the loess into secondary Fe oxides.

RESULTS AND DISCUSSION

Depth Profiles of Magnetic Properties

The depth plots of χ_{LF}, χ_{FD}, and χ_{ARM} (Fig. 2a–2c) show that the magnetic signals for the paleosol units are enhanced relative to the underlying loess, which can be ascribed to the pedogenic neoformation of fine-grained (SP plus SD) maghemite (Zhou et al., 1990; Forster et al., 1994; Maher et al., 2003; Liu et al., 2005). The values of these three magnetic parameters are systematically lower, however, in the peak paleosols below L6 (~40 m) than those above this unit.

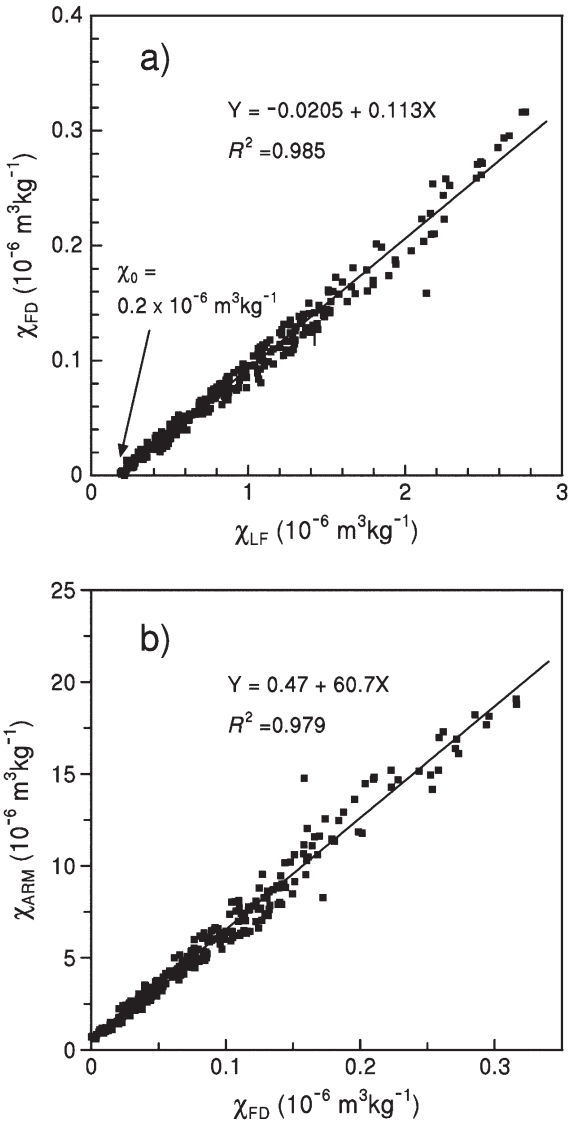

Fig. 3. Plots of (a) frequency-dependent magnetic susceptibility, χ_{FD}, against low-frequency magnetic susceptibility, χ_{LF}, and (b) anhysteretic remanent magnetization, χ_{ARM}, against χ_{FD}. The *x* axis intercept and *y* axis intercept of the regression lines in (a) and (b) are named χ_o (~0.2 × 10^{-6} m^3 kg^{-1}) and $\chi_{ARM,o}$ (~0.46 × 10^{-6} m^3 kg^{-1}), respectively, and are the estimates of χ_{FD} and χ_{ARM} contributed by aeolian inputs.

The χ_{FD}–χ_{LF} and the χ_{ARM}–χ_{FD} correlations are illustrated in Fig. 3a and 3b, respectively. Previous studies have shown that χ_{FD}% is determined mainly by the GSD of fine-grained magnetic particles in the SP and SD regions (Worm, 1998; Worm and Jackson, 1999). When the bulk susceptibility is relatively low, however, χ_{FD}% can also be seriously distorted by contributions from coarse-grained pseudo-single-domain (PSD) and multidomain (MD) magnetite, as well as by Fe silicates in the loess (Liu et al., 2004c). Such contributions can be estimated from the *x* axis intercept, χ_o, which represents contributions to the bulk χ from the parent material (Forster et al., 1994); for our profile, χ_o was 0.2 × 10^{-6} m^3 kg^{-1} (Fig. 3a). The same rationale can also be applied to χ_{ARM}. Although χ_{ARM} is sensitive to the concentration of SD magnetic particles, contributions from PSD and MD particles are

not negligible, especially in the unaltered loess and intermediate paleosol samples. The contribution of aeolian inputs to χ_{ARM} can be estimated from the *y* axis intercept in Fig. 3b.

Worm (1998) and Worm and Jackson (1999) showed that χ_{FD}% relates inversely to the width of the GSD of fine-grained particles. For many moderately weathered soils and paleosols, χ_{FD}% is 8 to 12% (Maher, 1988; Dearing et al., 1996), therefore pedogenic particles exhibit a relatively broad GSD. Our results (~11.3%; slope of the regression line in Fig. 3a) are consistent with those previous studies. The narrow range spanned by the χ_{FD}% values thus indicates that the GSD of pedogenic SP + SD maghemite is very similar across the studied sequence (Liu et al., 2005).

The use of biplots of χ_{ARM} and χ for magnetic granulometry is traditionally named the "King method" (Banerjee et al., 1981). The χ/χ_{ARM} ratio has later been used more often as a grain size proxy (dimensionless, or equivalently χ_{ARM}/χ). Stable SD particles exhibit the highest χ_{ARM}, but the lowest χ, yielding a minimum χ/χ_{ARM}. By contrast, both SP and PSD/MD particles exhibit a higher χ, but a lower χ_{ARM} SP particles are supposed to carry no remanence. Thus, higher χ/χ_{ARM} ratios are observed in these two cases.

The χ/χ_{ARM} ratio (0.33) for the parent loess can be estimated as $(\chi_o - \chi_{para})/\chi_{ARMo}$, where χ_{para} (~0.05×10^{-6} m^3 kg^{-1}; Liu et al., 2004b) is the susceptibility contributed by the paramagnetic background. The χ/χ_{ARM} ratio (0.145) for pedogenic maghemite particles is estimated as 1/(60.7 × 0.113), where 60.7 is the slope of the regression line (Fig. 3b) with a physical meaning of $(\chi_{ARM} - \chi_{ARMo})/\chi_{FD}$, and 0.113 the slope of the regression line in Fig. 3a. Clearly, aeolian inputs have a higher χ/χ_{ARM} ratio than pedogenic particles, consistent with the fact that the GSD of aeolian magnetite is coarser than that of pedogenic maghemite. For pedogenic particles, the χ/χ_{ARM} ratio (0.145) is higher than the typical 0.09 to 0.1 value found for stable SD particles (Maher, 1988). The difference (~0.045) is contributed by SP maghemites; therefore, the contribution of SD particles to the susceptibility enhancement is about twice (0.09/0.04 = 2) that of SP particles, which is consistent with data for samples from the last glacial–interglacial intervals (Liu et al., 2004b).

Low-Temperature Dependence of χ_{FD}

The room-temperature χ_{FD}% has limitations in representing the total concentration of SP particles because this parameter is sensitive only to viscous SP particles with size near the SP/SD threshold (Worm, 1998; Worm and Jackson, 1999). To determine the GSD of pedogenic maghemite particles, Liu et al. (2005) used the Néel theory and the low-temperature variations in χ_{FD}. At room temperature, SD particles (< ~100 nm) change their magnetic properties sharply around ~20 to 25 nm. For SD particles larger than this size threshold, susceptibility is independent of frequency because they are blocked. For SD particles much smaller than this threshold, susceptibility is also independent of frequency because the time constants for the susceptibility measurements are much larger than the relaxation time. Therefore, χ_{FD} peaks at the SD/SP threshold. As the temperature is lowered, a decrease in grain size occurs that corresponds to the maximum χ_{FD} value. Thus, temperature can be used as a window with a view to determining the grain size distribution of finer SP particles. In other words, the χ_{FD}–*T* curve can be taken as an analog of the GSD curve, even though there is a nonlinear transformation between grain size and temperature (Liu et al., 2005).

As can be seen in Fig. 4a, the χ_{FD}–*T* curves for three representative samples across the L6/S5 boundary are very similar. This suggests that the GSD of the pedogenically produced SP particles differs little among samples. Moreover, the χ_{FD}–*T* curves for these samples from the Luochuan section of the CLP (Fig. 4a) resemble those from sections in both the western and eastern parts of the CLP (Fig. 4b). Therefore, we can conclude that the GSD of pedogenic SP particles is independent of the degree of pedogenesis. Consequently, the room-temperature χ_{FD} is proportional to the concentration of these pedogenic SP particles, and thus can be confidently used as a proxy to quantify their relative concentration changes.

Various studies indicate that the pedogenic ferromagnetic particles consist of maghemite rather than magnetite (Fine et al., 1993; Verosub et al., 1993; Heller and Evans, 1995; Deng et al., 2000, 2001; Liu et al., 2003; Chen et al., 2005). One reason is that these fine-grained particles can be easily oxidized to maghemite due to their high surface-to-volume ratio regardless of their initial states (magnetite or maghemite) (van Velzen and Dekkers, 1999; Liu et al., 2003). To confirm this assumption, we selected 10 paleosol samples from the profile (two from S4, three from S5, one from S6, one from S7, and three from S8) and treated them with acid ammonium oxalate using the method of Schwertmann (1964). This extractant dissolves magnetite crystals of small (<100-nm) size as a result of the well-known catalytic effect of the Fe(II) in the dissolution (Reyes and Torrent, 1997; van Oorschot et al., 2002). Maghemite crystals of nanometric size, however, are dissolved to a relatively little extent (we found 30% dissolution for crystals of ~20 nm and <3% dissolution for crystals of 40 nm; unpublished data; see also Reyes and Torrent,1997). In the 10 paleosol samples studied, the oxalate treatment caused a 6 to 18% decrease in χ_{LF} (mean = 10%), but no significant change in χ_{FD}%. This result is consistent with the idea that the pedogenic ferrimagnets consist of maghemite rather than magnetite.

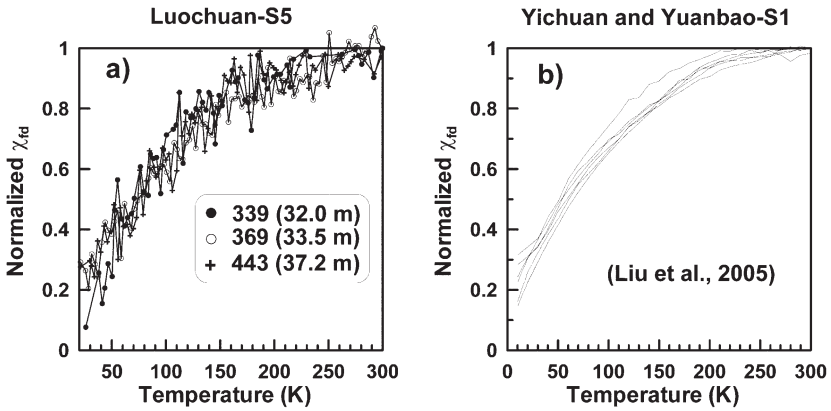

Fig. 4. Temperature dependence of frequency-dependent magnetic susceptibility, χ_{FD}, for (a) samples of S5 (this study, central Chinese Loess Plateau [CLP]), and (b) samples of S1 from Yuanbao (western CLP) and Yichuan (eastern CLP) (Liu et al., 2005).

In summary, the linear trends between χ_{FD}, χ_{LF}, and χ_{ARM} and the consistent low-*T* χ_{FD}–*T* behavior strongly suggest that the GSD of the pedogenic ferrimagnets is similar throughout the Luochuan section and ranges from the SP to SD grain region. The χ_{FD}% and the contribution of

SP and SD maghemites to the bulk susceptibility are both consistent with previous results for other loess profiles, which suggests that the genesis of these minerals has been uniform throughout the CLP. A recent study on modern loessic soil profiles from the midwestern USA (Geiss and Zanner, 2006) also exposed the similarity of the pedogenic ferrimagnetic component (which consisted of a mixture of SP, SD, and possible PSD particles). Thus, in terms of GSD, one consistent magnetic enhancement process functions across rather a wide range of precipitation conditions (Geiss and Zanner, 2006).

Depth Profiles of Hematite and Goethite

Figures 2d, 2e, and 2f show the depth distribution of hematite, goethite, and the Fe_d/Fe_t ratio, respectively. The concentration of Fe_t on a carbonate-free basis (not shown) was relatively constant (34–40 g kg^{-1}), which suggests that the parent loess was essentially homogeneous. By contrast, the concentration of Fe_d spanned a wider range (9–15 g kg^{-1}) as a result of the loess being weathered in the paleosol layers. Based on the Fe_d/Fe_t ratio, the less weathered layers are the L4, L5, L6, and L9 loess units, with Fe_d/Fe_t = ~0.24; on a carbonate-free basis, this corresponds to a background Fe_d concentration in the region of 7.5 g kg^{-1}, and background hematite and goethite concentrations of approximately 4 and 7 g kg^{-1}, respectively. A moderately high correlation exists between Fe_d/Fe_t and χ_{FD} ($Fe_d/Fe_t = 0.239 + 0.367\chi_{FD}$; $R^2 = 0.531$; $n = 53$, $P < 0.001$). This indicates that weathering of the loess Fe-bearing minerals (mainly Fe chlorite; Ji et al., 2006) has resulted in the formation of significant amounts of fine-grained ferrimagnets.

The hematite concentration ranges from 2.9 to 11.2 g kg^{-1} (3.6–11.2 g kg^{-1} on a carbonate-free basis) and its depth distribution is roughly parallel to that of χ_{LF} and χ_{FD}; therefore, Hm and χ_{FD} are highly correlated ($Hm = 3.53 + 28.8\chi_{FD}$; $R^2 = 0.825$; $n = 53$, $P < 0.001$; Fig. 5a). If we now consider that the concentration of pedogenic hematite, ΔHm, is the $Hm - Hm_0$ difference, where Hm_0 is the *y* axis intercept—which provides an estimate for the hematite concentration at $\chi_{FD} = 0$, i.e., in the background loess, then the previous correlation simply indicates that $\Delta Hm/\chi_{FD}$ is essentially constant throughout the profile. The concentration of goethite, Gt, ranges from 6.3 to 11.8 g kg^{-1} (7.2–11.8 g kg^{-1} on a carbonate-free basis). In contrast to hematite, Gt, or ΔGt (i.e., the concentration of pedogenic goethite as calculated similarly to ΔHm) is only weakly correlated with χ_{FD} ($R^2 = 0.09$; $P < 0.05$; Fig. 5b). Accordingly, the correlation between Fe_d and χ_{FD} adopts an intermediate R^2 value ($Fe_d = -0.219 + 0.0319\chi_{FD}$; $R^2 = 0.754$; $n = 53$, $P < 0.001$).

The differences in hematite and goethite concentrations between the paleosol and the background loess suggest that pedogenesis resulted in the formation of more hematite than goethite, consistent with the positive correlation between Hm/(Hm + Gt) and Fe_d/Fe_t [$Hm/(Hm + Gt) = 0.0144 + 1.44Fe_d/Fe_t$; $R^2 = 0.36$; $n = 53$, $P < 0.001$].

Balsam et al. (2004) reported similar goethite concentrations, but hematite concentrations two to three times lower than those of Fig. 2 (~1.6 g kg^{-1} for the loess units and ~3.4 g kg^{-1} for the S5 paleosol peak). The difference can be tentatively attributed to the standard used by these researchers (a synthetic hematite) rather than to the diffuse reflectance method they used for quantification (described in Ji et al., 2002). The idea that the nature of the standard resulted in underestimated hematite concentrations is supported by Fig. 2 in Ji et al. (2002), where the combined Fe contents in hematite and goethite was about 20 to 30% lower than Fe_d in the calibration samples.

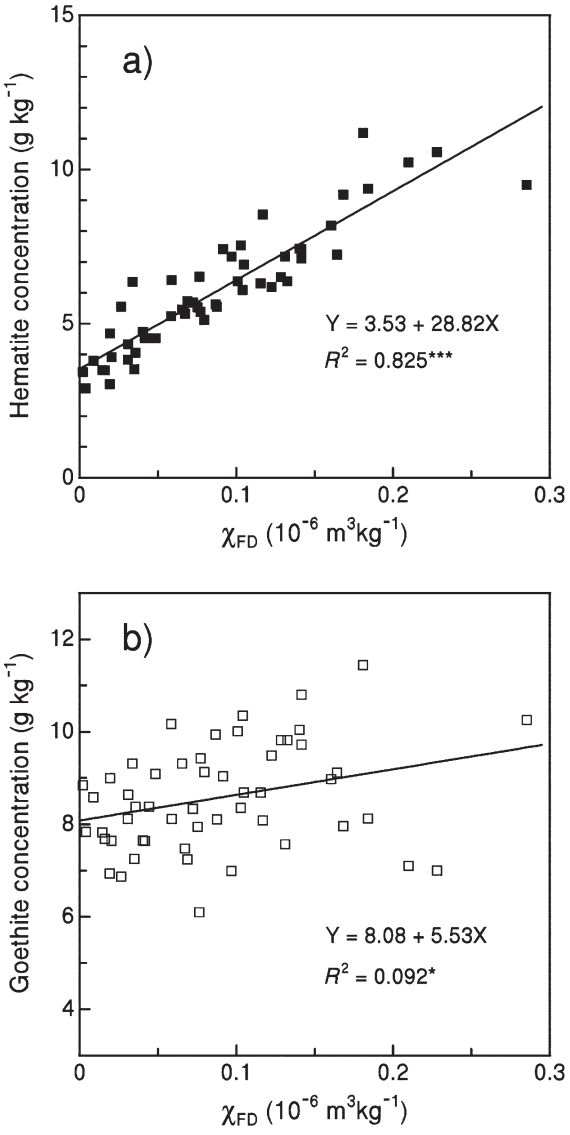

Fig. 5. Relationships between (a) the concentration of hematite and frequency-dependent magnetic susceptibility, χ_{FD}; and (b) the concentration of goethite and χ_{FD}.

Relationships between Maghemite, Hematite, and Goethite

The high correlation between χ_{FD}—a proxy for the concentration of pedogenic maghemite—and the hematite concentration supports the hypothesis of Torrent et al. (2006) that maghemite is an intermediate product in the ferrihydrite to hematite transformation in aerobic soils. This model implies that various ligands are sorbed on the surface of ferrihydrite particles, which are thus "blocked" and can undergo internal rearrangement and slow dehydroxylation to hematite via maghemite (Barrón and Torrent, 2002; Barrón et al., 2003). The experiments of Barrón and Torrent (2002) revealed complete conversion of maghemite to hematite at temperatures above 100°C. Should this model be applicable to soil environments, one could expect a gradual increase in the hematite/maghemite ratio with weathering and progress of the ferrihydrite → maghemite

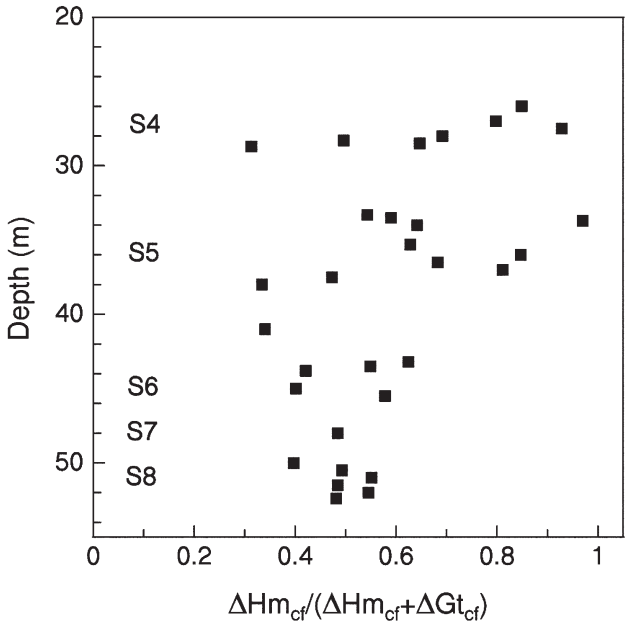

Fig. 6. The ratio of carbonate-free pedogenic hematite, ΔHm_{cf}, and goethite, ΔGt_{cf}, concentrations, as $\Delta Hm_{cf}/(\Delta Hm_{cf} + \Delta Gt_{cf})$, in the paleosol samples where dithionite-extractable Fe/total Fe >0.26.

→ hematite transformation, which is rarely the case (Torrent et al., 2006). It is therefore likely that part of the maghemite formed does not evolve to hematite, the partitioning between maghemite and hematite depending on the particular soil environment. For instance, maghemite would tend to be stabilized in the presence of large concentrations of blocking ligands. The soil environment is also likely to determine the fraction of the precursor ferrihydrite that is directly transformed to hematite, as suggested by synthesis experiments in ligand-poor media (Barrón and Torrent, 2002); in fact, irrespective of the synthesis conditions, some hematite particles are always formed at the earlier stages of the ferrihydrite transformation. In any case, the high correlation between the pedogenic maghemite and hematite concentrations supports the hypothesis that these two minerals form concomitantly.

A soil environment favoring dissolution of ferrihydrite and further polymerization of the Fe^{3+} ions in solution in turn favors the formation of goethite, which predominates in soils that are cool, moist, and rich in organic matter (Schwertmann, 1985). The previous considerations led to the well-established idea that the Hm/(Hm + Gt) ratio largely reflects the nature of the environment in which pedogenic Fe oxides have formed, and can thus be used as a paleoenvironmental indicator.

Based on the ferrihydrite → maghemite → hematite model, χ_{FD} is influenced, among other factors, by (i) conditions favoring the blocking of ferrihydrite by some ligands and its further transformation into maghemite and hematite—less pedogenic maghemite is generally found in aerobic, hematite-free soils relative to similar hematite-containing soils (Torrent et al., 2006), and (ii) the rate and duration of weathering of the primary Fe-bearing minerals, which determine the amount of precursor ferrihydrite. This obviously limits the usefulness of χ_{FD} as the sole paleoclimatic indicator. A multiproxy approach based on magnetic properties, color, Fe_d/Fe_t ratio, and other pedogenetic indices is thus required (Vidic et al., 2004). Specifically, as discussed below, the parallel variation of χ_{FD} and the hematite concentration in the Luochuan profile makes it reasonable to support any paleoclimatic reconstruction on the Hm/(Hm + Gt) ratio as well.

Based on the Fe_d/Fe_t ratio, the paleosols above 40 m (S4 and S5) are more weathered on average than are those below this depth, which may be the result of differences in paleoclimate or pedogenesis duration. The differences in Fe_d/Fe_t are not reflected in significant differences in the Hm/χ_{FD} ratio between the two groups of paleosols, however. This suggests that the nature of the processes leading to the concomitant formation of maghemite and hematite was essentially similar for both groups.

To further compare the two paleosol groups, we used the $\Delta Hm_{cf}/(\Delta Hm_{cf} + \Delta Gt_{cf})$ ratio, where ΔHm_{cf} and ΔGt_{cf} represent the concentrations of pedogenic hematite and goethite, respectively. They were calculated as $(Hm_{cf} - Hm_{cf0})$ and $(Gt_{cf} - Gt_{cf0})$, where Hm_{cf} and Gt_{cf} are the respective carbonate-free concentrations of hematite and goethite in the sample, and Hm_{cf0} and Gt_{cf0} are the lowest values of these concentrations in the parent loess. The depth profile of the ratio is shown in Fig. 6, where only the samples with Fe_d/Fe_t >0.26 were plotted to exclude weakly weathered soil samples. The ratio is significantly larger in the paleosols above 40 m (S4 and S5) than in those below such a depth (S6–S8). One cannot ascribe the difference to the higher degree of weathering (due, for example, to a longer pedogenesis) in S4 and S5 because no correlation exists between the $\Delta Hm_{cf}/(\Delta Hm_{cf} + \Delta Gt_{cf})$ ratio and Fe_d/Fe_t—which is a good proxy for the degree of weathering. It must then be concluded that the paleosols above 40 m developed in an environment that was more favorable to the formation of hematite than those below it.

The simplest hypothesis accounting for this fact is that both paleotemperature and paleorainfall were higher above 40 m than below such a depth, which resulted not only in a higher degree of weathering, but also in a higher $\Delta Hm_{cf}/(\Delta Hm_{cf} + \Delta Gt_{cf})$ ratio, as it is well established that an increase in temperature favors hematite over goethite (Schwertmann, 1985). Since present and past climates in the CLP have been governed by alternations in the warm, moist southwest summer monsoon and the dry, cool northwest winter monsoon, an increase in paleorainfall is likely to be associated with an increase in temperature. This hypothesis is consistent with the observed differences in marine benthic $\delta^{18}O$ and $\delta^{13}C$ records, which suggest strengthened summer monsoons in S4 and S5 relative to S6 to S8 (Guo et al., 2000).

Our results point to the usefulness of the hematite–goethite relationship as a paleoclimatic indicator for the loess–paleosol sections, consistent with previous studies (Vidic et al., 2004; Balsam et al., 2004). Unlike other useful pedological indicators (e.g., the absolute hematite and goethite concentrations, χ_{FD}, Fe_d/Fe_t, and Rb/Sr), the ratio of pedogenic hematite to goethite is likely to be relatively independent of the duration of pedogenesis, as suggested by data for various soil chronosequences (Torrent, 1976; Torrent et al., 1980).

Unresolved Questions

A long-sustained hypothesis is that biotic or abiotic formation of fine-grained magnetite (Maher, 1998; Maher et al., 2003, and references therein; Chen et al., 2005), which is later oxidized to maghemite, contributes substantially to the soil magnetic enhancement. Significant reduction of Fe(III) to Fe(II), however one strict requirement for magnetite formation is unlikely to occur in well-

drained soils, where hematite can form and substantial magnetic enhancement can develop. In somewhat imperfectly drained soils, where the Fe^{2+} needed for the formation of magnetite is likely to appear in the solution during the wet season, little magnetic enhancement occurs and goethite rather than hematite is formed. Consequently, the coexistence of pedogenic magnetite (whether oxidized to maghemite or not) and hematite in the Chinese loess paleosols is paradoxical in the light of that hypothesis. Such a paradox does not exist in the ferrihydrite → maghemite → hematite model because maghemite not magnetite and hematite are products at different stages of a consistent transformation process. Moreover, a biotic origin is inconsistent with the weak correlation found between total N, a proxy for organic matter and hence biotic activity in soil, and χ_{FD} ($R^2 = 0.204$; $P < 0.01$). Indeed, we cannot exclude the possibility of magnetite forming under microanaerobic environments in otherwise well-drained soils, as suggested by some electron microscopy studies (e.g., Chen et al., 2005). The relative significance of this pathway, however, remains to be established, particularly in magnetically enhanced soil horizons where organic compounds—the main electron donors for the reduction of Fe(III)—are present at low concentrations.

The goethite concentration in the least altered loess samples is about 2.5 times higher than that of hematite (i.e., the parent loess contains more goethite than hematite). Because aeolian inputs were transported from the source regions by Asian winter monsoons, the higher initial goethite contents might reflect the fact that more goethite was formed in the source region or during the transportation process during cold periods. Confirming this hypothesis would require further research into the spatial distribution of goethite and, especially, the goethite content of the parent material in the source region.

One other question is the relationship between hematite and maghemite. Our conceptual model predicts that both minerals formed through the same pedogenic pathway. If that were the case, we could expect them to exhibit some crystallochemical similarities (e.g., substitution of foreign ions for Fe). More elaborate experiments that were not performed in this study are needed to check this assumption. Finally, the coexistence of hematite and maghemite, and SD maghemite and SP maghemite, requires testable hypotheses on which factors affect the rates of the transformation steps in the pathway from ferrihydrite to hematite.

CONCLUSIONS

Although magnetic enhancement in the loess–paleosol Luochuan profile can, in principle, be governed by many factors, a fairly simple scenario emerges from the almost constant GSD of pedogenic fine-grained maghemite and the linear relationship between pedogenic hematite and maghemite. Magnetic enhancement can be ascribed to an increase in concentration in fine-grained (SP + SD) maghemite, which seems to be an intermediate product in the pedogenic transformation of ferrihydrite to hematite. The concentration of pedogenic goethite is poorly correlated with the concentrations of the other pedogenic Fe oxides, probably because there is no genetic relationship between the formation of goethite on the one hand and maghemite–hematite on the other. The ratio of pedogenic hematite to goethite in the different paleosols seems to have been influenced by the nature of the paleoclimate rather than by substantial differences in the degree and duration of pedogenic weathering.

ACKNOWLEDGMENTS

This work was partly funded by Spain's Ministerio de Ciencia y Tecnología, Project AGL2003–01510. Q.S. Liu was supported by a European Commission Marie-Curie Fellowship (IIF), Proposal no. 7555. J. Bloemendal was supported by the UK Natural Environment Research Council.

REFERENCES

Balsam, W., B. Ellwood, and J.F. Ji. 2005. Direct correlation of the marine oxygen isotope record with the Chinese Loess Plateau iron oxide and magnetic susceptibility records. Palaeogeogr. Palaeoclimatol. Palaeoecol. 221:141–152.

Balsam, W., J.F. Ji, and J. Chen. 2004. Climatic interpretation of the Luochuan and Lingtai loess sections, China, based on changing iron oxide mineralogy and magnetic susceptibility. Earth Planet. Sci. Lett. 223:335–348.

Banerjee, S.K., J. King, and J. Marvin. 1981. A rapid method for magnetic granulometry with applications to environmental studies. Geophys. Res. Lett. 8:333–336.

Barrón, V., and J. Torrent. 2002. Evidence for a simple pathway to maghemite in Earth and Mars soils. Geochim. Cosmochim. Acta 66:2801–2806.

Barrón, V., J. Torrent, and E. de Grave. 2003. Hydromaghemite, an intermediate in the hydrothermal transformation of 2-line ferrihydrite into hematite. Am. Mineral. 88:1679–1688.

Bigham, J.M., R.W. FitzPatrick, and D.G. Schulze. 2002. Iron oxides. p. 323–366. *In* J.B. Dixon and D.G. Schulze (ed.) Soil mineralogy with environmental applications. SSSA Book Ser. 7. SSSA, Madison, WI.

Bloemendal, J., and X.M. Liu. 2005. Rock magnetism and geochemistry of two plio-pleistocene Chinese loess–palaeosol sequences: Implications for quantitative palaeoprecipitation reconstruction. Palaeogeogr. Palaeoclimatol. Palaeoecol. 226:149–166.

Boyle, J.F. 2000. Rapid elemental analysis of sediment samples by isotope source XRF. J. Paleolimnol. 23:213–221.

Bronger, A. 2003. Correlation of loess–paleosol sequences in East and Central Asia with SE Central Europe: Towards a continental Quaternary pedostratigraphy and paleoclimatic history. Quat. Int. 106–107:11–31.

Chen, T., H. Xu, Q. Xie, J. Chen, J. Ji, and H. Lu. 2005. Characteristics and genesis of maghemite in Chinese loess and paleosols: Mechanism for magnetic susceptibility enhancement in paleosols. Earth Planet. Sci. Lett. 240:790–802.

Cornell, R.M., and U. Schwertmann. 2003. The iron oxides. 2nd ed. John Wiley & Sons, Weinheim, Germany.

Dearing, J.A., R.J.L. Dann, K. Hay, J.A. Lees, P.J. Loveland, B.A. Maher, and K. O'Grady. 1996. Frequency-dependent susceptibility measurements of environmental materials. Geophys. J. Int. 124:228–240.

Deng, C.L., J. Shaw, Q.S. Liu, Y.X. Pan, and R.X. Zhu. 2006. Mineral magnetic variation of the Jingbian loess/paleosol sequence in the northern Loess Plateau of China: Implications for Quaternary development of Asian aridification and cooling. Earth Planet. Sci. Lett. 241:248–259.

Deng, C.L., R. Zhu, M.J. Jackson, K.L. Verosub, and M.J. Singer. 2001. Variability of the temperature-dependent susceptibility of the Holocene eolian deposits in the Chinese loess plateau: A pedogenesis indicator. Phys. Chem. Earth 26A: 873–878.

Deng, C.L., R.X. Zhu, K.L. Verosub, M.J. Singer, and B.Y. Yuan. 2000. Paleoclimatic significance of the temperature-dependent susceptibility of Holocene loess along a NW–SE transect in the Chinese loess plateau. Geophys. Res. Lett. 27:3715–3718.

Dunlop, D.J., and Ö. Özdemir. 1997. Rock magnetism: Fundamentals and frontiers. Cambridge Univ. Press, New York.

Fassbinder, J.W.E., H. Stanjek, and H. Vali. 1993. Occurrence of magnetic bacteria in soil. Nature 343:161–163.

Fine, P., M.J. Singer, R. La Ven, K.Verosub, and R.J. Southard. 1989. Role of pedogenesis in distribution of magnetic susceptibility in two California chronosequences. Geoderma 44:287–306.

Fine, P., M.J. Singer, K.L. Verosub, and J. TenPas. 1993. New evidence for the origin of ferrimagnetic minerals in loess from China. Soil Sci. Soc. Am. J. 57:1537–1542.

Forster, T., M.E. Evans, and F. Heller. 1994. The frequency dependence of low field susceptibility in loess sediments. Geophys. J. Int. 118:636–642.

Geiss, C.E., and C.W. Zanner. 2006. How abundant is pedogenic magnetite? Abundance and grain size estimates for loessic soils based on rock magnetic

analyses. J. Geophys. Res. 111:B12S21, doi:10.1029/2006JB004564.
Guo, Z.T., P. Biscaye, L.Y. Wei, X.H. Chen, S.Z. Peng, and T.S. Liu. 2000. Summer monsoon variations over the last 1.2 Ma from the weathering of loess–soil sequences in China. Geophys. Res. Lett. 27:1751–1754.
Heller, F., and M.E. Evans. 1995. Loess magnetism. Rev. Geophys. 33:211–240.
Heller, F., and T.S. Liu. 1984. Magnetism of Chinese loess deposits. Geophys. J. R. Astron. Soc. 77:125–141.
Heller, F., and T.S. Liu. 1986. Palaeoclimatic and sedimentary history from magnetic susceptibility of loess in China. Geophys. Res. Lett. 13:1169–1172.
Ji, J.F., W. Balsam, J. Chen, and L.W. Liu. 2002. Rapid and quantitative measurement of hematite and goethite in the Chinese loess–paleosol sequence by diffuse reflectance spectroscopy. Clays Clay Miner. 50:210–218.
Ji, J.F., L. Zhao, W. Balsam, J. Chen, T. Wu, and L.W. Liu. 2006. Detecting chlorite in the Chinese loess sequence by diffuse reflectance spectroscopy. Clays Clay Miner. 54:266–273.
Kukla, G., F. Heller, X.M. Liu, T.C. Xu, T.S. Liu, and Z.S. An. 1988. Pleistocene climates in China dated by magnetic susceptibility. Geology 16:811–814.
Liu, Q.S., S.K. Banerjee, M.J. Jackson, F.H. Chen, Y.X. Pan, and R.X. Zhu. 2003. An integrated study of the grain-size-dependent magnetic mineralogy of the Chinese loess/paleosol and its environmental significance. J. Geophys. Res. 108(B9):2437, doi:10.1029/2002JB002264.
Liu, Q.S., S.K. Banerjee, M.J. Jackson, C.L. Deng, Y.X. Pan, and R.X. Zhu. 2004a. New insights into partial oxidation model of magnetites and thermal alteration of magnetic mineralogy of the Chinese loess in air. Geophys. J. Int. 158:506–514.
Liu, Q.S., S.K. Banerjee, M.J. Jackson, B.A. Maher, C.L. Deng, Y.X. Pan, and R.X. Zhu. 2004b. Mechanism of the magnetic susceptibility enhancements of the Chinese loess. J. Geophys. Res. 109:B12107, doi:10.1029/2004JB003249.
Liu, Q.S., M.J. Jackson, Y.J. Yu, F.H. Chen, C.L. Deng, and R.X. Zhu. 2004c. Grain size distribution of pedogenic magnetic particles in Chinese loess/paleosols. Geophys. Res. Lett. 31:L22603, doi:10.1029/2004GL021090.
Liu, Q.S., J. Torrent, B.A. Maher, Y. Yu, C.L. Deng, R.X. Zhu, and X.X. Zhao. 2005. Quantifying grain size distribution of pedogenic magnetic particles in Chinese loess and its significance for pedogenesis. J. Geophys. Res. 110:B11102, doi:10.1029/2005JB003726.
Lovley, D.R., J.F. Stolz, J.L. Nord, and E.J.P. Phillips. 1987. Anaerobic production of magnetite by a dissimilatory iron-reducing microorganism. Nature 330:252–254.
Maher, B.A. 1988. Magnetic properties of some synthetic submicron magnetites. Geophys. J. 94:83–96.
Maher, B.A. 1998. Magnetic properties of modern soils and Quaternary loessic paleosols: Paleoclimatic implications. Palaeogeogr. Palaeoclimatol. Palaeoecol. 137:25–54.
Maher, B.A., A. Alekseev, and T. Alekseeva. 2003. Magnetic mineralogy of soils across the Russian steppe: Climatic dependence of pedogenic magnetite formation. Palaeogeogr. Palaeoclimatol. Palaeoecol. 201:321–341.
Maher, B.A., and R.M. Taylor. 1988. Formation of ultrafine magnetite in soils. Nature 336:368–370.
Maher, B.A., and R. Thompson. 1992. Paleoclimatic significance of the mineral magnetic record of the Chinese loess and paleosols. Quat. Res. 37:155–170.
Maher, B.A., R. Thompson, and L.P. Zhou. 1994. Spatial and temporal reconstructions of changes in the Asian palaeomonsoon—a new mineral magnetic approach. Earth Planet. Sci. Lett. 125:461–471.
Mehra, O.P., and M.L. Jackson. 1960. Iron oxide removal from soils and clays by a dithionite–citrate system buffered with sodium bicarbonate. Clays Clay Miner. 7:317–327.
Reyes, I., and J. Torrent. 1997. Citrate–ascorbate as a highly selective extractant for poorly crystalline iron oxides. Soil Sci. Soc. Am. J. 61:1647–1654.
Scheinost, A.C., A. Chavernas, V. Barrón, and J. Torrent. 1998. Use and limitations of the second-derivative diffuse reflectance spectroscopy in the visible to near-infrared range to identify and quantify Fe oxide minerals in soils. Clays Clay Miner. 46:528–536.
Schwertmann, U. 1964. Differenzierung der Eisenoxide des Bodens durch Extraktion mit Ammoniumoxalat-Lösung. Z. Pflanzenernaehr. Dueng. Bodenkd. 105:194–202.
Schwertmann, U. 1985. The effect of pedogenic environments on iron oxide minerals. Adv. Soil Sci. 1:172–200.
Torrent, J. 1976. Soil development in a sequence of river terraces in northern Spain. Catena 3:137–151.
Torrent, J., V. Barrón, and Q.S. Liu. 2006. Magnetic enhancement is linked to and precedes hematite formation in aerobic soil. Geophys. Res. Lett. 33: L02401, doi:10.1029/2005GL024818.
Torrent, J., U. Schwertmann, and D.G. Schulze. 1980. Iron oxide mineralogy of some soils of two river terrace sequences in Spain. Geoderma 25:191–208.
van Oorschot, I.H.M., M.J. Dekkers, and P. Havlicek. 2002. Selective dissolution of magnetic iron oxides with the acid-ammonium-oxalate/ferrous-iron extraction technique: II. Natural loess and palaeosol samples. Geophys. J. Int. 149:106–117.
van Velzen, A.J., and M.J. Dekkers. 1999. Low-temperature oxidation of magnetite in loess–paleosol sequences: A correction of rock magnetic parameters. Stud. Geophys. Geod. 43:357–375.
Verosub, K.L., P. Fine, M.J. Singer, and J. TenPas. 1993. Pedogenesis and paleoclimate: Interpretation of the magnetic susceptibility record of Chinese loess–paleosol sequences. Geology 21:1011–1014.
Vidic, N.A., M.J. Singer, and K.L. Verosub. 2004. Duration dependence of magnetic susceptibility enhancement in the Chinese loess–paleosols of the past 620 ky. Palaeogeogr. Palaeoclimatol. Palaeoecol. 211:271–288.
Vidic, N.A., and K.L. Verosub. 1999. Magnetic properties of soils of the Ljubljana Basin chronosequence, Slovenia. Chin. Sci. Bull. 44(Suppl. 1):75–80.
Worm, H.U. 1998. On the superparamagnetic-stable single domain transition for magnetite, and frequency dependency of susceptibility. Geophy. J. Int. 133:201–206.
Worm, H.U., and M. Jackson. 1999. The superparamagnetism of Yucca Mountain Tuff. J. Geophys. Res. 104:25415–25425.
Zhou, L.P., F. Oldfield, A.G. Wintle, S.G. Robinson, and J.T. Wang. 1990. Partly pedogenic origin of magnetic variations in Chinese loess. Nature 346:737–739.